Maternal *Sall4* Is Indispensable for Epigenetic Maturation of Mouse Oocytes

Kai Xu[1,6], Xia Chen[1,6], Hui Yang[1], Yiwen Xu[2], Yuanlin He[3], Chenfei Wang[1], Hua Huang[4], Baodong Liu[4], Wenqiang Liu[1], Jingyi Li[1], Xiaochen Kou[1], Yanhong Zhao[1], Kun Zhao[1], Linfeng Zhang[1], Zhenzhen Hou[1], Hong Wang[1], Hailin Wang[4], Jing Li[3], Hengyu Fan[2], Fengchao Wang[5], Yawei Gao[1], Yong Zhang[1], Jiayu Chen[1*], Shaorong Gao[1*]

[1] Clinical and Translational Research Center of Shanghai First Maternity and Infant Hospital, Shanghai Key Laboratory of Signaling and Disease Research, School of Life Sciences and Technology, Tongji University, Shanghai 200092, China, [2] Life Sciences Institute and Innovation Center for Cell Signaling Network, Zhejiang University, Hangzhou 310058, China, [3] State Key Laboratory of Reproductive Medicine, Department of Histology and Embryology, Nanjing Medical University, Nanjing 210029, China, [4] The State Key Laboratory of Environmental Chemistry and Ecotoxicology, Research Center for Eco-Environmental Sciences, Chinese Academy of Sciences, Beijing 100085, China, [5] National Institute of Biological Sciences, NIBS, Beijing 102206, China, [6] These authors contributed equally to this work.

Running title: *SALL4 regulates oocyte epigenetic maturation*

*To whom correspondence should be addressed: Shaorong Gao, Ph.D., 1239 Siping Road, Shanghai 200092, China; Telephone: 86-21-65982278; Fax: 86-21-65985182; E-mail: gaoshaorong@tongji.edu.cn or Jiayu Chen Ph.D., 1239 Siping Road, Shanghai 200092, China; Telephone: 86-21-65982276; Fax: 86-21-65982276; E-mail: chenjiayu@tongji.edu.cn

Keywords: *Sall4*; oocyte epigenetic maturation; oogenesis; DNA methylation; histone modification.

ABSTRACT

Splat-like 4 (*Sall4*) plays important roles in maintaining pluripotency of embryonic stem cells and in various developmental processes. Here, we find that *Sall4* is highly expressed in oocytes and early embryos. To investigate the roles of SALL4 in oogenesis, we generated *Sall4* maternal specific knockout mice by using CRISPR/Cas9 system. And we find that the maternal deletion of *Sall4* causes developmental arrest of oocytes at germinal vesicle stage with non-surrounded nucleus and the subsequent meiosis resumption is prohibited. We further discover that the loss of maternal *Sall4* causes failure in establishment of DNA methylation in oocytes. Furthermore, we find that *Sall4* modulates H3K4me3 and H3K27me3 modifications by regulating the expression of key histone demethylases coding genes *Kdm5b*, *Kdm6a* and *Kdm6b* in oocytes. Moreover, we demonstrate that the aberrant H3K4me3 and H3K27me3 cause mis-expression of genes that are critical for oocytes maturation and meiosis resumption. Taken together, our study explores a pivotal role of *Sall4* in regulating epigenetic maturation of mouse oocytes.

In mammals, oocyte maturation is an important developmental process, which is prerequisite for the subsequent fertilization and embryo development. In mice, oocytes reside in the ovarian follicles and follicles can be devided into 5 stages according to the developmental

process: primordial follicle, primary follicle, secondary follicle, early antral follicle and antral follicle (1). During this process, the oocyte will undergo maturation as the follicle grows into antral follicle. Then the mature oocyte acquires the ability to resume meiosis with its nucleus forming surrounded-nuclear (SN) conformation and the transcription quiescence occuring simultaneously.

The oocyte maturation encompasses the following three main processes: nuclear maturation, cytoplasmic maturation and epigenetic maturation. Comparing to the nuclear and cytoplasmic maturation, the underlying mechanism of oocyte epigenetic maturation is not fully understood. Previous studies have indicated that DNA methylation and histone modifications play functional roles in oocytes maturation. *De novo* DNA methylation starts to occur in the secondary follicle oocytes, and completes when oocytes acquire the competence of resuming meiosis (2). Among all the DNA methyltransferases (DNMTs), DNMT3A and DNMT3L are mainly responsible for the establishment of DNA methylome in oocytes (3). Meanwhile, as another important epigenetic modification, histone modifications have been demonstrated important for chromosome organization, chromosome segregation and meiotic resumption during oocytes maturation (4). However, it remains elusive how histone modifications are regulated and to what extent the transcriptome is influenced during oocytes maturation.

SALL4, as a zinc-finger protein, was first identified in *Drosophila*. In humans, *SALL4* mutations cause Okihiro syndrome with multiple organs developmental abnormalities (5). In mice, *Sall4* is primarily expressed in early embryos, embryonic stem cells (ESCs), primordial germ cells (PGCs) and germ cells with different and specific functions. *Sall4* null embryos die shortly after implantation on embryonic day 6.5 (E6.5) (6). In ESCs, *Sall4* can activate the pluripotent master gene *Pou5f1* (7) and recruit nucleosome remodeling and deacetylase (NuRD) complex to suppress the trophectoderm marker *Cdx2* (8). Other studies have shown that SALL4 acts as an epigenetic regulator in ESCs by recruiting DNMTs, HDAC1 and HDAC2 to methylate CpG islands and deacetylate the histone tails in active chromatin regions (9). In germ cell development, *Sall4* plays essential roles in ensuring the correct specification and migration of PGCs (10). In male mice, SALL4 interacts with PLZF and promotes the specification of spermatogonial progenitor cells (SPCs) (11). However, whether *Sall4* functions in oogenesis remains unknown.

In the present study, we aimed to investigate if the maternal *Sall4* plays a role in oocyte maturation and subsequent totipotency establishment. We first confirmed that *Sall4* is highly expressed in oocytes at different developmental stages. Then, we investigated the function and mechanism of SALL4 in oogenesis by specifically deleting *Sall4* in oocytes. Our results indicate that maternal SALL4 functions as an epigenetic modulator and plays an essential role in the epigenetic maturation of oocytes.

RESULTS

Characterization of SALL4 in Oogenesis and Pre-implantation Embryo Development - We first identified the expression pattern of *Sall4* in oogenesis by conducting quantitative real-time polymerase chain reaction (qRT-PCR) and immunofluorescence (IF) staining. *Sall4* expression begins in primary follicle stage oocytes, and continues accumulating as the oocytes grow (**Figure 1A and B**). During this period, SALL4 was localized in the nucleus (**Figure 1B**). When germinal vesicle breakdown (GVBD) occurs, SALL4 diffuses into the cytoplasm (**Figure 1E**

MII). After fertilization, SALL4 aggregates in the pronuclei but dramatically degenerates during the first cleavage. Then, SALL4 re-expressed and accumulated until the formation of blastocyst (**Figure 1D and E**). The live cell imaging of oocytes collected from *Sall4*-mCherry transgenic mice further confirmed this expression and localization pattern of SALL4 (**Figure 1C and F**). These results imply that SALL4 may be a maternal factor and play important roles in oogenesis and pre-implantation embryo development.

Maternal Sall4 Knockout Oocytes Are Immature - To identify the effects of maternal SALL4 in oogenesis, we first generated *Sall4*$^{fl/fl}$ mice using CRISPR/Cas9 system. By crossing with *Zp3-Cre* or *Gdf9-Cre* transgenic mice, we then obtained *Sall4*$^{fl/fl}$*;Zp3-Cre* and *Sall4*$^{fl/fl}$*;Gdf9-Cre* mice in which *Sall4* was deleted specifically in primary follicle stage or primordial follicle stage oocytes, respectively (**Figure 2A**). The knockout effects were validated by immunohistochemistry (IHC), genotyping, western blotting and IF staining (**Figure 3A and Figure 2B-D**). Subsequently we found that both *Sall4*$^{fl/fl}$*;Zp3-Cre* and *Sall4*$^{fl/fl}$*;Gdf9-Cre* female mice were infertile (**Table 1**). Furthermore, hematoxylin and eosin (H&E) staining indicated that antral follicles were absent in ovaries of both genotypes (**Figure 3A and F**). Apart from histological results, the non-SN conformation and high transcription activity in SALL4 null oocytes further indicated that they were immature (**Figure 3B and C**). Moreover, to identify whether SALL4 null oocytes were partially competent to resume meiosis, we co-cultured the WT or SALL4 null oocytes with WT granulosa cells *in vitro* for 16 hours**.** The results showed that SALL4 null oocytes could not undergo GVBD (**Figure 3D and E**), indicating that SALL4 null oocytes were not even partially mature.

SALL4 Is Essential for de novo DNA Methylation by Interacting with DNMT3A - To identify the mechanism of SALL4 in oocyte maturation, we first focused on the factors interacting with SALL4. IF staining showed that the contents and localization of NuRD complex core components and DNMT3B were not altered in SALL4 null oocytes (**Supplemental Figure 1A-C**). Surprisingly, the nuclear localization of DNMT3A was obviously lost in SALL4 null oocytes (**Figure 4A**). And the IF staining for 5-methylcytosine (5mC) showed that the SALL4 null oocytes were hypomethylated (**Figure 4B**). Furthermore, by using an ultrasensitive ultra-high performance liquid chromatography-electrospray ionization-quadrople mass spectrometry (UHPLC-MS/MS) approach for absolute quantification analysis of 5mC demonstrated that the DNA methylation levels in SALL4 null oocytes was about 75% lower than WT oocytes (**Figure 4C**). To obtain a detailed DNA methylation profile of SALL4 null oocytes, we performed reduced representation bisulfite sequencing (RRBS) using secondary follicle (SF) stage and early antral follicle (EAF) stage oocytes from *Sall4*$^{fl/fl}$*;Zp3-Cre* mice and *Sall4*$^{fl/fl}$ mice separately. The result showed that the whole genome of SALL4 null oocytes were extensively hypomethylated. Moreover, the maternal germ cell differentially methylated regions (gDMRs) and imprinting control regions (ICRs) were barely methylated. In addition, the repeated elements were also hypomethylated (**Figure 4D**). The bisulfite sequencing PCR on maternal gDMRs (*Igf2r* and *Mcst2*) and repetitive sequence regions (*Line1* and *IAP-LTR*) further confirmed the results of RRBS analysis (**Figure 4E**). Therefore, the loss of SALL4 can cause *de novo* DNA methylation failure probably by influencing the nuclear deposition of DNMT3A.

The Transcriptome of SALL4 Null Oocytes Is Dramatically Perturbed - To further verify why

SALL4 null oocytes can not undergo maturation, we performed single-cell RNA sequencing on secondary follicle (SF) and early antral follicle (EAF) stage oocytes from *Sall4$^{fl/fl}$;Zp3-Cre* and *Sall4$^{fl/fl}$* mice, respectively. The RNA-Seq results showed that more than 4,000 genes were mis-expressed in SALL4 null oocytes (**Figure 5A and B**). Specifically, SALL4 null SF and EAF stage oocytes showed 2,230 down-regulated genes (with 973 genes overlapped) and 2,030 up-regulated genes (with 738 genes overlapped) (**Figure 5C and D**). Then we conducted gene ontology (GO) analysis on the overlapped differentially expressed genes. There were a lot of phosphorylation and oxidative stress response related genes were highly expressed in SALL4 null oocytes. The transmission electron microscopy analysis also showed that the SALL4 null oocytes have much thinner zona pellucida, abnormal mitochondria and endoplasmic reticulum (**Supplemental Figure 2A**). Whereas the down-regulated genes in SALL4 null oocytes were mainly chromosome organization, transcription regulation and cell cycle related (**Figure 5E**). Above all, SALL4 null oocytes showed obvious disorders in metabolism, transcriptome and epigenome. Moreover, the aberrant expression of cell cycle related genes can partially explain why SALL4 null oocytes can't undergo GVBD. We then analyzed the correlation between the transcriptome disorders and DNA methylome abnormalities by comparing gene expression levels and methylation levels of gene promoter regions. In SALL4 null oocytes, the hypomethylated or hypermethylated genes relative to WT oocytes showed no correlation with gene expression levels (**Figure 5F**), which indicates that DNA methylation cannot explain the transcriptome disorders in SALL4 null oocytes.

SALL4 Modulates H3K4me3 and H3k27me3 by Regulating Kdm5b, Kdm6a and Kdm6b - In view of the extensive and dramatic alteration of transcriptome in SALL4 null oocytes, we inferred that SALL4 might regulate transcription through modulating some other epigenetic modifications. Therefore, we combined the published SALL4 ChIP-Seq data (GSE73390) (12) with our RNA-Seq data to screen histone modification related genes which are regulated by SALL4. Then we focused on several histone lysine demethylase coding genes: *Kdm5b*, *Kdm6a* and *Kdm6b*. In detail, the abnormal high expression level of *Kdm5b*, as well as the low expression levels of *Kdm6a* and *Kdm6b* in SALL4 null oocytes were confirmed by qRT-PCR (**Figure 6A**). Besides, ChIP-Seq data and luciferase reporter assays showed SALL4 bound primarily at the promoter of these genes (**Figure 6B and Supplemental Figure 2B**). Correspondingly, the level of H3K4me3 was lower and the level of H3K27me3 was higher in SALL4 null oocytes compared to WT oocytes (**Figure 6C and D, Supplemental Figure 3A**). Thus, we hypothesized that the abnormalities of H3K4me3 and H3K27me3 levels might account for the transcriptome disorders in SALL4 null oocytes. To validate this hypothesis, we then injected *Kdm5b* mRNA and siRNAs targeting *Kdm6a* and *Kdm6b* together into postnatal day 10 (P10) WT oocytes, which was set as the experimental group. For control group oocytes, GFP mRNA and scramble siRNAs were injected. IF staining results demonstrated that the oocytes in experimental group could mimic the changes of H3K4me3 and H3K27me3 observed in SALL4 null oocytes (**Figure 7A**). After *in vitro* culture and maturation induction, the GVBD rate of oocytes was calculated. The results showed that about 70% oocytes could undergo GVBD in control group, whereas, the GVBD rate in experimental group was only 25% (**Figure 7B and C**). Moreover, RNA-Seq analysis was conducted on oocytes randomly collected from both

experimental and control group separately. Then we analyzed the functions of overlapped mis-expressed genes in both the experimental group oocytes and the SALL4 null oocytes, and found that the overlapped mis-expressed genes were mainly related to responses of hormone stimulations and cell surface linked signal transduction (**Figure 7D**). Among these genes, glial cell-derived neurotrophic factor (GDNF) family receptor alfha1 (*Gfra1*) was well studied in oogenesis. During oocytes maturation, human chorionic gonadotropin (hCG) stimulates the granulosa cells to secret GDNFs, which further induce the oocytes to grow and mature (13,14). Loss-of-function experiment have also proved the essential roles of *Gfra1* in successful fertilization of oocytes (15). Moreover, the platelet derived growth factor alpha (*Pdgfa*) and prolactin receptor (*Prlr*) have been reported to be essential for oocyte maturation by their functions in oocytes-granulosa cells interactions (16,17). In addition, the down-regulation of mechanistic target of rapamycin (*Mtor*) and homeobox A7 (*Hoxa7*) has been shown to be detrimental to oocyte growth (18,19).To further verify whether these oogenesis related genes are regulated by H3K4me3 and H3K27me3 levels, we performed ChIP-qPCR assays. Because of the shortage of oocytes, we applied ultra-low input ChIP-qPCR to investigate the levels of H3K4me3 and H3K27me3 on the promoter regions of *Gfra1*, *Pdgfa*, *Prlr*, *Mtor* and *Hoxa7*. The results showed that the H3K4me3 levels on the promoters of these genes in SALL4 null oocytes are much lower than in the WT oocytes (**Figure 7E upper panel**). And the H3K27me3 levels on the promoters of these genes in SALL4 null oocytes are much higher than in the WT oocytes (**Figure 7E lower panel**). Therefore, we can conclude that H3K4me3 and H3K27me3 regulate the expression of *Gfra1*, *Pdgfa*, *Prlr*, *Mtor* and *Hoxa7* in oocytes. Above all, we verified that the proper levels of H3K4me3 and H3K27me3 guard the normal transcriptome, which are critical for oocyte-granulosa cell interactions and oocyte growth.

DISCUSSION

Recent studies have revealed DNA regions with non-methylated H3K4 and tri-methylated H3K36 are preferentially methylated (20,21). However, although the histone modifications in SALL4 null oocytes (low levels of H3K4me3 and high levels of H3K36me3 (**Figure 6E and Supplemental Figure 3A**) are propitious for DNA methylation establishment, without SALL4, the *de novo* methylation still failed. Such contrary results have also been found in HDAC1/2 knockout oocytes (22,23). Thus *de novo* DNA methylation may also rely on specific factors apart from histone modifications. Furthermore, SALL4, HDAC1 and HDAC2 are all related to NuRD complex, which promotes us to put forward a hypothesis that NuRD complex may take parts in *de novo* DNA methylation during oogenesis.

In the microinjection experiment, there were still 25% oocytes which could undergo GVBD. One possible reason was the follicles used for microinjection were obtained from P10.5 mice, however, SALL4 depletion occurred at P6.5 or earlier in *Sall4*$^{fl/fl}$*;Zp3-Cre* mice. Besides, SALL4, as an important transcription factor, definitely can directly regulate other genes which play roles in oocyte maturation. Even though, the microinjection experiment still powerfully validated the proper levels of H3K4me3 and H3K27me3 were important for regulating transcriptome in oogenesis and were essential for oocytes maturation. Due to the limited materials, previous studies mainly focused on how histone marks influenced the nuclear conformation, which are convenient to observe. Yet, how histone marks modulated transcriptome in oogenesis was less studied. In our study, we interpreted how

H3K4me3 and H3K27me3 modulated transcription of certain genes which were essential for oocytes maturation by oocytes microinjection, single-cell RNA-Seq assays and ultra-low input ChIP-qPCR.

In summary, we found that oocyte-specific *Sall4* knockout mice showed severe defects in oogenesis including impaired follicle development and meiosis resumption inhibition. We demonstrated that SALL4 null oocytes showed a severely abnormal transcriptome and aberrant epigenome including failure in DNA methylation establishment and histone modifications abnormalities. As for DNA methylation, SALL4 was indispensable for the nuclear localization of DNMT3A and thus essential for DNA methylation establishment in the process of oocytes maturation. As for histone modifications, SALL4 regulated the expression of *Kdm5b*, *Kdm6a* and *Kdm6b*, which then modulated the levels of H3K4me3 and H3K27me3. In turn, the abnormal H3K4me3 and H3K27me3 modifications led to mis-expression of many key genes essential for oocytes maturation (**Supplemental Figure 3B**). Overall, our present study elucidated a pivotal role of pluripotency factor, *Sall4*, in epigenetic maturation of mouse oocytes.

EXPERIMENTAL PROCEDURES

Mice generation and maintenance - *Sall4*$^{fl/fl}$ mice and *Sall4-mCherry* mice were generated using CRISPR/Cas9 system. All experiments were performed in accordance with the University of Health Guide for the Care and Use of Laboratory Animals and were approved by the Biological Research Ethics Committee of Tongji University.

Oocytes and early embryos collection and culture - Primordial, primary, secondary, early antral and antral follicles were obtained from *Sall4*$^{fl/fl}$, *Sall4*$^{fl/fl}$*;Zp3-Cre* female mice at P2.5, P6.5, P12.5, P17.5 and P22.5 as previously described (24). Fully-grown oocytes were isolated from 4-6 weeks old mice 46 hours after PMSG injection. Zygotes were obtained from the ampulla of the uterine tube of superovulated female mice after mating with male mice. Then, 2 cell, 4 cell, 8 cell, morula and blastocyst embryos were obtained by culturing zygotes in Quinn's Advantage medium (*In Vitro* Fertilization, Inc.).

SN/GVBD ratio calculation and statistics – For SN/non-SN ratio calculation, we obtained oocytes from P21.5 *Sall4*$^{fl/fl}$ and *Sall4*$^{fl/fl}$*;Zp3-Cre* female mice. Then we use Hoechst 33258 (Thermo Fisher Scientific) to stain the nucleus DNA. Then we observed the nucleus of oocytes under fluorescence microscope and counted the oocytes in SN or non-SN conformation. Three independent experiments were performed for each WT and KO groups. For GVBD ratio calculation, we obtained oocytes from P21.5 *Sall4*$^{fl/fl}$ and *Sall4*$^{fl/fl}$*;Zp3-Cre* female mice, and then cultured these oocytes *in vitro* for 16 hours. Then we observed the germinal vesicles of each oocytes. Then we counted the amount of oocytes with or without germinal vesicles. The experiments were conducted for three times independently.

Immunofluorescent staining - For immunofluorescent staining, collected oocytes and embryos were fixed in 4% paraformaldehyde for 15 min and then permeabilized for 15 min in 0.3% Triton X-100. For 5mC staining, an additional 30 min of 4N HCl treatment and three times washes in Tris (PH8.0) were needed. The samples were blocked in PBS with 2.5% BSA. Then, they were incubated with the primary antibodies. Next, the samples were washed and incubated with secondary antibodies. After washed in PBS and incubated with DAPI, the samples were observed under confocal microscope.

BrUTP incorporation assay - Oocytes obtained from P21.5 *Sall4*$^{fl/fl}$ or *Sall4*$^{fl/fl}$*;Zp3-Cre* mice were injected with 5mM BrUTP (Sigma).

Then the oocytes were washed three times and cultured in the incubator (37°C，5%CO_2). 25 min later, the oocytes were fixed and proceeded to IF staining for BrUTP.

Bisulfite sequencing PCR - Approximately 200 EAF stage WT or KO oocytes were used for genomic DNA isolation with the QIAamp DNA Micro Kit (Qiagen). Then DNA was treated with the MethylCode Bisulfite Conversion Kit (Invitrogen). Next, EpiTect Whole Bisulfitome Kit (Qiagen) was used to amplify the converted genome. Then, nested PCRs was performed to amplify the gDMR regions of the indicated genes. The amplified products were cloned into vectors with the pEASY™-T5 Zero cloning kit (TransGen Biotech), ten to sixteen randomly selected clones were sequenced in Genewiz, Inc. Primers used in this analysis are listed in **Table 2**.

UHPLC-MRM-QQQ analysis for oocytes - Sample preparation prior to the UHPLC-MS/MS analysis was operated as described previously (25). The analysis was performed on an Agilent 1290 Infinity ultrahigh performance LC system coupled with an Agilent QQQ6490 mass spectrometer equipped with a jet stream electrospray ionization source (Santa Clara). The mass spectrometer was operated under positive ionization with multiple reactions monitoring (MRM) mode.

Oocytes microinjection and in vitro maturation - We detached secondary follicles from P10.5 WT female mice ovaries. We randomly separated the follicles into two groups, and then we injected siRNAs and mRNAs into the oocytes using microinjection facilities. Next, the follicles were cultured in medium as previously reported (26). After 10 day's culture, the oocytes were stripped from follicles and released into modified M2 medium containing 10% FBS and 100 ng/ml FSH for oocytes maturation.

Single-cell RNA-Seq library generation - Single oocyte was transferred into lysate buffer. Then the Single-cell RNA-Seq libraries were generated followed previously published studies (27,28). Then Paired-end 125-bp sequencing were further performed on HiSeq 2000 at the Berry Genomics Corporation.

Single-cell RRBS library generation - The Single-cell RRBS libraries were generated followed previously published study (29). Paired-end 125-bp sequencing were further performed on HiSeq 2000 at the Berry Genomics Corporation.

Quantitative RT-PCR analysis - Total RNA from oocytes and embryos was purified using the Arcturus PicoPure RNA Isolation Kit (Applied biosystems). The cDNA was synthesized by a reverse transcription system using 5×All-In-One RT MasterMix (ABM). Quantitative RT-PCR was performed using SYBR Green master mix (Vazyme, Nanjing, China). Primers used are shown in **Table 2**. Primers were synthesized at Genewiz, Inc.

RNA-Seq and RRBS analysis - All RNA-Seq reads were mapped and quantified as previously described (30,31). The number of mapped reads was counted using htseq-count (v 0.6.0) (32). Differential expression analysis was conducted by edgeR (v 3.10.2) using read counts. Genes with a Benjamini and Hochberg-adjusted P value (FDR) < 0.05 and a mean fold change of > 1 were termed differentially expressed. Among all the RNA-Seq data, SF WT group have two replicates, SF KO group, EAF WT group and EAF KO group all have three replicates. All the RRBS Sequencing reads were mapped as previously described (33,34). The methylation level of each CpG site was estimated using mcall (v 1.3.0) with default parameters, and CpG sites with read depths ≥ 1 were counted as total CpG coverage of the sample. The bisulfite conversion ratio for each sample was calculated using unmethylated CpGs divided by total CpGs detected in the lambda genome. Among

all the RRBS data, SF WT group have 7replicates, SF KO group have 5 replicates, EAF WT group have 4 replicates, and EAF KO group have 2 replicates.

Ultra-low input ChIP-qPCR - For Ultra-low input ChIP-qPCR, 600 oocytes were used per reaction. All oocytes were washed three times in 0.5% BSA-PBS (Sigma) solution to avoid any possible contamination. The procedure of ULI-NChIP was carried out as previously described (35). One µg of histone H3K4me3 antibody (Cell signaling Technology, #9727) or one ug of histone H3K27me3 antibody (Diagnode, pAb-069-050) was used for each immunoprecipitation reaction. Then we use 3ng/ul DNA obtained from the ChIP experiments and 10ng/ul input DNA for ChIP-qPCR analysis. The primers used in the qPCR experiment are listed in **Table 2**. There are two replicates each for H3K4me3 WT group, H3K4me3 KO group, H3K27me3 WT group and H3K27me3 KO group.

ACKNOWLEDGEMENTS

We thank Dr. Youqiang Su from Nanjing Medical University and Dr. Qingyuan Sun from Institute of zoology, Chinese Academy of Sciences for their comments. We thank Dr. Zhi Liu and Dr. Xiling Du from Tongji University for analyzing oocytes by electron microscope. The data supporting the RNA-Seq and RRBS analysis have been uploaded to NCBI GEO database GSE84924.

CONFLICT OF INTEREST

The authors declare that they have no conflict of interest with the content of this article.

AUTHOR CONTRIBUTIONS

K.X. and X.C. performed most of the experiments. H.Y., Y.X., Y.H., C.W., B.L., W.L., J.Y.L., X.K., Y.Z., K.Z., L.Z., Z.H., H.W., J.L., H.F., F.W., Y.G. and Y.Z. helped with experiments and data analysis. K.X., X.C., J.C., and S.G. designed the research, analyzed data and wrote the paper.

REFERENCES

1. van den Hurk, R., and Zhao, J. (2005) Formation of mammalian oocytes and their growth, differentiation and maturation within ovarian follicles. *Theriogenology* **63**, 1717-1751
2. Smallwood, S. A., Tomizawa, S., Krueger, F., Ruf, N., Carli, N., Segonds-Pichon, A., Sato, S., Hata, K., Andrews, S. R., and Kelsey, G. (2011) Dynamic CpG island methylation landscape in oocytes and preimplantation embryos. *Nature genetics* **43**, 811-814
3. Kaneda, M., Okano, M., Hata, K., Sado, T., Tsujimoto, N., Li, E., and Sasaki, H. (2004) Essential role for de novo DNA methyltransferase Dnmt3a in paternal and maternal imprinting. *Nature* **429**, 900-903
4. Gu, L., Wang, Q., and Sun, Q. Y. (2010) Histone modifications during mammalian oocyte maturation: dynamics, regulation and functions. *Cell cycle* **9**, 1942-1950
5. Al-Baradie, R., Yamada, K., St Hilaire, C., Chan, W. M., Andrews, C., McIntosh, N., Nakano, M., Martonyi, E. J., Raymond, W. R., Okumura, S., Okihiro, M. M., and Engle, E. C. (2002) Duane radial ray syndrome (Okihiro syndrome) maps to 20q13 and results from mutations in SALL4, a new member of the SAL family. *American journal of human genetics* **71**, 1195-1199
6. Sakaki-Yumoto, M., Kobayashi, C., Sato, A., Fujimura, S., Matsumoto, Y., Takasato, M., Kodama, T., Aburatani, H., Asashima, M., Yoshida, N., and Nishinakamura, R. (2006) The murine homolog of SALL4, a causative gene in Okihiro syndrome, is essential for embryonic stem cell proliferation, and cooperates with Sall1 in anorectal, heart, brain and kidney development. *Development* **133**, 3005-3013
7. Zhang, J., Tam, W. L., Tong, G. Q., Wu, Q., Chan, H. Y., Soh, B. S., Lou, Y., Yang, J., Ma, Y., Chai, L., Ng, H. H., Lufkin, T., Robson, P., and Lim, B. (2006) Sall4 modulates embryonic stem cell pluripotency and early embryonic development by the transcriptional regulation of Pou5f1. *Nature cell biology* **8**, 1114-1123
8. Yuri, S., Fujimura, S., Nimura, K., Takeda, N., Toyooka, Y., Fujimura, Y., Aburatani, H., Ura, K., Koseki, H., Niwa, H., and Nishinakamura, R. (2009) Sall4 is essential for stabilization, but not for pluripotency, of embryonic stem cells by repressing aberrant trophectoderm gene expression. *Stem cells* **27**, 796-805
9. Yang, J., Corsello, T. R., and Ma, Y. (2012) Stem cell gene SALL4 suppresses transcription through recruitment of DNA methyltransferases. *The Journal of biological chemistry* **287**, 1996-2005
10. Yamaguchi, Y. L., Tanaka, S. S., Kumagai, M., Fujimoto, Y., Terabayashi, T., Matsui, Y., and

Nishinakamura, R. (2015) Sall4 is essential for mouse primordial germ cell specification by suppressing somatic cell program genes. *Stem cells* **33**, 289-300

11. Hobbs, R. M., Fagoonee, S., Papa, A., Webster, K., Altruda, F., Nishinakamura, R., Chai, L., and Pandolfi, P. P. (2012) Functional antagonism between Sall4 and Plzf defines germline progenitors. *Cell stem cell* **10**, 284-298
12. Lovelace, D. L., Gao, Z., Mutoji, K., Song, Y. C., Ruan, J., and Hermann, B. P. (2016) The regulatory repertoire of PLZF and SALL4 in undifferentiated spermatogonia. *Development* **143**, 1893-1906
13. Dole, G., Nilsson, E. E., and Skinner, M. K. (2008) Glial-derived neurotrophic factor promotes ovarian primordial follicle development and cell-cell interactions during folliculogenesis. *Reproduction* **135**, 671-682
14. Kawamura, K., Ye, Y., Kawamura, N., Jing, L., Groenen, P., Gelpke, M. S., Rauch, R., Hsueh, A. J., and Tanaka, T. (2008) Completion of Meiosis I of preovulatory oocytes and facilitation of preimplantation embryo development by glial cell line-derived neurotrophic factor. *Developmental biology* **315**, 189-202
15. Agopiantz, M., Xandre-Rodriguez, L., Jin, B., Urbistondoy, G., Ialy-Radio, C., Chalbi, M., Wolf, J. P., Ziyyat, A., and Lefevre, B. (2016) Growth arrest specific 1 (Gas1) and glial cell line-derived neurotrophic factor receptor a1 (Gfra1), two mouse oocyte glycosylphosphatidylinositol-anchored proteins, are involved in fertilisation. *Reproduction, fertility, and development* 10.1071/RD15367.
16. Sleer, L. S., and Taylor, C. C. (2007) Platelet-derived growth factors and receptors in the rat corpus luteum: localization and identification of an effect on luteogenesis. *Biology of reproduction* **76**, 391-400
17. Bole-Feysot, C., Goffin, V., Edery, M., Binart, N., and Kelly, P. A. (1998) Prolactin (PRL) and its receptor: actions, signal transduction pathways and phenotypes observed in PRL receptor knockout mice. *Endocrine reviews* **19**, 225-268
18. Huntriss, J., Hinkins, M., and Picton, H. M. (2006) cDNA cloning and expression of the human NOBOX gene in oocytes and ovarian follicles. *Molecular human reproduction* **12**, 283-289
19. Lopez, E., Berna-Erro, A., Lopez, J. J., Granados, M. P., Bermejo, N., Brull, J. M., Salido, G. M., Rosado, J. A., and Redondo, P. C. (2015) Role of mTOR1 and mTOR2 complexes in MEG-01 cell physiology. *Thrombosis and haemostasis* **114**, 969-981
20. Ciccone, D. N., Su, H., Hevi, S., Gay, F., Lei, H., Bajko, J., Xu, G., Li, E., and Chen, T. (2009) KDM1B is a histone H3K4 demethylase required to establish maternal genomic imprints. *Nature* **461**, 415-418
21. Stewart, K. R., Veselovska, L., Kim, J., Huang, J., Saadeh, H., Tomizawa, S., Smallwood, S. A., Chen, T., and Kelsey, G. (2015) Dynamic changes in histone modifications precede de novo DNA methylation in oocytes. *Genes & development* **29**, 2449-2462
22. Ma, P., de Waal, E., Weaver, J. R., Bartolomei, M. S., and Schultz, R. M. (2015) A DNMT3A2-HDAC2 Complex Is Essential for Genomic Imprinting and Genome Integrity in Mouse Oocytes. *Cell reports* **13**, 1552-1560
23. Ma, P., Pan, H., Montgomery, R. L., Olson, E. N., and Schultz, R. M. (2012) Compensatory functions of histone deacetylase 1 (HDAC1) and HDAC2 regulate transcription and apoptosis during mouse oocyte development. *Proceedings of the National Academy of Sciences of the United States of America* **109**, E481-489
24. Pedersen, T., and Peters, H. (1968) Proposal for a classification of oocytes and follicles in the mouse ovary. *Journal of reproduction and fertility* **17**, 555-557

25. Yin, R., Mao, S. Q., Zhao, B., Chong, Z., Yang, Y., Zhao, C., Zhang, D., Huang, H., Gao, J., Li, Z., Jiao, Y., Li, C., Liu, S., Wu, D., Gu, W., Yang, Y. G., Xu, G. L., and Wang, H. (2013) Ascorbic acid enhances Tet-mediated 5-methylcytosine oxidation and promotes DNA demethylation in mammals. *Journal of the American Chemical Society* **135**, 10396-10403
26. Pfender, S., Kuznetsov, V., Pasternak, M., Tischer, T., Santhanam, B., and Schuh, M. (2015) Live imaging RNAi screen reveals genes essential for meiosis in mammalian oocytes. *Nature* **524**, 239-242
27. Tang, F., Barbacioru, C., Wang, Y., Nordman, E., Lee, C., Xu, N., Wang, X., Bodeau, J., Tuch, B. B., Siddiqui, A., Lao, K., and Surani, M. A. (2009) mRNA-Seq whole-transcriptome analysis of a single cell. *Nature methods* **6**, 377-382
28. Tang, F., Barbacioru, C., Bao, S., Lee, C., Nordman, E., Wang, X., Lao, K., and Surani, M. A. (2010) Tracing the derivation of embryonic stem cells from the inner cell mass by single-cell RNA-Seq analysis. *Cell stem cell* **6**, 468-478
29. Guo, H., Zhu, P., Guo, F., Li, X., Wu, X., Fan, X., Wen, L., and Tang, F. (2015) Profiling DNA methylome landscapes of mammalian cells with single-cell reduced-representation bisulfite sequencing. *Nature protocols* **10**, 645-659
30. Trapnell, C., Pachter, L., and Salzberg, S. L. (2009) TopHat: discovering splice junctions with RNA-Seq. *Bioinformatics* **25**, 1105-1111
31. Trapnell, C., Williams, B. A., Pertea, G., Mortazavi, A., Kwan, G., van Baren, M. J., Salzberg, S. L., Wold, B. J., and Pachter, L. (2010) Transcript assembly and quantification by RNA-Seq reveals unannotated transcripts and isoform switching during cell differentiation. *Nat Biotechnol* **28**, 511-515
32. Anders, S., Pyl, P. T., and Huber, W. (2015) HTSeq--a Python framework to work with high-throughput sequencing data. *Bioinformatics* **31**, 166-169
33. Xi, Y., and Li, W. (2009) BSMAP: whole genome bisulfite sequence MAPping program. *BMC bioinformatics* **10**, 232
34. Guo, W., Fiziev, P., Yan, W., Cokus, S., Sun, X., Zhang, M. Q., Chen, P. Y., and Pellegrini, M. (2013) BS-Seeker2: a versatile aligning pipeline for bisulfite sequencing data. *BMC Genomics* **14**, 774
35. Brind'Amour, J., Liu, S., Hudson, M., Chen, C., Karimi, M. M., and Lorincz, M. C. (2015) An ultra-low-input native ChIP-seq protocol for genome-wide profiling of rare cell populations. *Nat Commun* **6**, 6033

FOOTNOTES

This work was supported by the National Natural Science Foundation of China (31401247, 31325019, 31430056, 91319306, 31471392, 31401266, 31401247, 31501196，31501197 and 31501183), the Ministry of Science and Technology of China (2016YFA0100400, 2015CB964800, 2015CB964503, 2014CB964601, and 2012CBA01300), and the Science and Technology Commission of Shanghai Municipality (15XD1503500，YF1403900 and 14CG16).

Table 1: Both *Sall4$^{fl/fl}$;Zp3-Cre* and *Sall4$^{fl/fl}$;Gdf9-Cre* were infertile.

	Sall4$^{fl/fl}$	*Sall4$^{fl/fl}$;Zp3-Cre*	*Sall4$^{fl/fl}$;Gdf9-Cre*
number of breedings	15	0	0
total number of pups	133	0	0
pups per breeding	8.87	0	0

Table 2: Primers for qRT-PCR, bisulfite sequencing and ChIP-qPCR primers

Kdm6a	F	CGGGCGGACAAAAGAAGAAC
	R	CATAGACTTGCATCAGATCCTCC
Kdm5b	F	AAGCCAAGCTCTGTTCAGCAA
	R	GAAGGCAATCGTTCTTCTCACT
Kdm6b	F	TGAAGAACGTCAAGTCCATTGTG
	R	TCCCGCTGTACCTGACAGT
Mest-outer	F	GATTTGGGATATAAAAGGTTAATGAG
	R	TCATTAAAAACACAAACCTCCTTTAC
Mest-inner	F	TTTTAGATTTTGAGGGTTTTAGGTTG
	R	AATCCCTTAAAAATCATCTTTCACAC
Igf2r-outer	F	TTAGTGGGGTATTTTTATTTGTATGG
	R	AAATATCCTAAAAATACAAACTACAC
Igf2r-inner	F	GTGTGGTATTTTTATGTATAGTTAGG
	R	AAATATCCTAAAAATACAAACTACAC
H19-outer	F	GAGTATTTAGGAGGTATAAGAATT
	R	ATCAAAAACTAACATAAACCCCT
H19-inner	F	GTAAGGAGATTATGTTTATTTTTGG
	R	CCTCATTAATCCCATAACTAT
Line 1-outer	F	GTTAGAGAATTTGATAGTTTTTGGAATAGG
	R	CCAAAACAAAACCTTTCTCAAACACTATAT
Line 1-inner	F	TAGGAAATTAGTTTGAATAGGTGAGAGGT
	R	TCAAACACTATATTACTTTAACAATTCCCA
Lap-LTR-outer	F	TTGATAGTTGTGTTTTAAGTGGTAAATAAA
	R	AAAACACCACAAACCAAAATCTTCTAC
Lap-LTR-inner	F	TTGTGTTTTAAGTGGTAAATAAATAATTTG
	R	CAAAAAAAACACACAAACCAAAAT
Gfra1	F	CTCCTCTGGCCACTCAAAGTTA
	R	TCCAGGTTGGGTCGGAACT
Hoxa7	F	CAGGGGTAGATGCGGAAACT
	R	GCGCCTCCTACGACCAAAAC

Mtor	F	GAAGCCGCCTGTCTGAACC
	R	CTAAATGCTCCACGGAAGGC
Pdgfa	F	AGAGCTTGAAACAGGTAGCCGA
	R	CTGCGGATACCTCGCCCAT
Prlr	F	GTGCTCGTGAGACAAAGGTAAC
	R	GAAAAATAGTCCCATCCCCCAGG

FIGURE LEGENDS

FIGURE 1. SALL4 expression pattern in the process of postnatal oocytes maturation and early embryo development.

(A) Quantitative RT-PCR analysis of *Sall4* mRNA (*Sall4a* and *Sall4b* variants) levels in oocytes at indicated follicle stages. The *Sall4* expression values were calculated relative to *Gapdh*. Data represent mean ± SEM, n=3

(B) IF staining for SALL4 in oocytes at indicated follicle stages. Scale bars, 20 μm.

(C) Live imaging for SALL4-mCherry in oocytes at indicated follicle stages. Scale bars, 20 μm.

(D) Quantitative RT-PCR analysis of *Sall4* mRNA (*Sall4a* and *Sall4b* variants) levels in pre-implantation embryos. The *Sall4* expression values were calculated relative to *Gapdh*. Data represent mean ± SEM, n=3.

(E) IF staining for SALL4 in pre-implantation embryos. Scale bars, 20 μm.

(F) Live imaging for SALL4-mCherry in pre-implantation embryos. Scale bars, 20 μm.

FIGURE 2. Generation of *Sall4* oocyte-specific knockout mice and their phenotypes.

(A) Schematic of strategy for generating *Sall4$^{fl/fl}$;Zp3-Cre* and *Sall4$^{fl/fl}$;Gdf9-Cre* mice. LA, left homologous arm. RA, right homologous arm. P1 and P2 are primers used for genotyping.

(B) Genotyping of *Sall4* knockout oocytes. The oocytes used for genotyping in the Lane2 to a Lane4 were obtained from *Sall4$^{fl/fl}$;Zp3-Cre* mice, whereas the oocytes in Lane 5 and Lane 6 were from *Sall4$^{fl/fl}$* mice. All the oocytes used were at EAF stage.

(C and D) Knockout validation of *Sall4$^{fl/fl}$;Zp3-Cre* oocytes by western blotting and IF staining. All the oocytes used were at EAF stage.

FIGURE 3. SALL4-null oocytes are immature.

(A) H&E and SALL4 IHC staining in P21.5 WT and two kinds of knockout mice ovaries. Scale bars, 100 μm.

(B) The SN/non-SN rate of oocytes in P21.5 WT and *Sall4$^{fl/fl}$;Zp3-Cre* (hereinafter referred to as KO) mice. Data represent mean ± SEM, n=3.

(C) BrUTP immunofluorescence staining results of WT and KO oocytes after injection of BrUTP for 25 min. The oocytes were obtained from *Sall4$^{fl/fl}$* mice and *Sall4$^{fl/fl}$;Zp3-Cre* mice, and the mice were injected with PMSG and HCG following the standard superovulation procedure. Scale bars, 10 μm.(D) Morphology of oocytes derived from WT and KO mice. The left two panels showed oocytes before *in vitro* culture, and the right two panels showed oocytes after maturation induction. The WT oocytes showed GVBD obviously and polar bodies could be seen in parts of oocytes (arrow pointed), whereas the germinal vesicles remained in KO oocytes. Scale bars, 50 μm.

(E) GVBD rate of WT and KO oocytes after *in vitro* maturation. Each experiment was conducted in triplicates. Data represent mean ± SEM, n=3.

(F) Numbers of follicles of indicated stages in *Sall4$^{fl/fl}$*, *Sall4$^{fl/fl}$;Zp3-Cre* and *Sall4$^{fl/fl}$;Gdf9-Cre* mice at P22.5 (46 hours after treatment of PMSG). Data represent mean ± SEM, n=3.

FIGURE 4. *De novo* DNA methylation in SALL4 null oocytes.

(A) DNMT3A IF staining in WT and KO EAF stage oocytes. DNMT3A signal was obviously lost in nuclear of KO oocytes. Scale bars, 20 μm.
(B) 5mC IF staining of EAF stage WT and KO oocytes. WT oocytes possessed a much higher signal than KO oocytes. Scale bars, 20μm.
(C) UHPLC-MS/MS analysis of 5mC content in EAF stage WT and KO oocytes. Data represent mean ± SEM, n=6 (***) P<0.001, Student's *t*-test.
(D) Box plots analysis showed the DNA methylation levels in various genomic regions. Data were obtained by RRBS analysis of SF and EAF oocytes WT and KO oocytes.
(E) Bisulfite sequencing PCR analysis of DNA methylation at *Igfr2*, *Mcst2*, *Line1* and *IAP-LTR* in WT and KO oocytes. Open circles, filled circles and cross represent unmethylated, methylated and undetected CpG sites respectively. The proportion of methylation levels was indicated below.

FIGURE 5. Transcriptome and methylome analysis of SALL4 null oocytes
(A and B) Heat map of differently expressed genes in SF and EAF stage KO oocytes comparing to WT oocytes data.
(C and D) Venn diagrams of down-regulated or up-regulated genes in KO oocytes. The overlapped regions show the genes both down-regulated and up-regulated in SF and EAF stages. The percentage and number of genes were indicated.
(E) Significant GO terms found in up-regulated or down-regulated genes in *Sall4*$^{fl/fl}$*;Zp3-Cre* oocytes at both SF and EAF stages.
(F) Correlation analysis between DNA methylome and trancriptome in oocytes. The box plots showed the expression levels of indicated genes in *Sall4*$^{fl/fl}$ (WT) and *Sall4*$^{fl/fl}$*;Zp3-Cre* (KO) oocytes. The genes analyzed in left panels are hypermethylated in *Sall4* knockout oocytes. The genes analyzed in right panels are hypomethylaed in *Sall4* knockout oocytes.

FIGURE 6. Histone modification of SALL4 null oocytes.
(A) qRT-PCR results for the expression of *Kdm5b, Kdm6a* and *Kdm6b* in EAF stage WT and KO oocytes. The expression levels of each gene are normalized with the expression levels of WT oocytes.
(B) SALL4 ChIP-Seq peaks in *Kdm5b, Kdm6a* and *Kdm6b* genes loci. Red boxes indicate the peaks in the promoter regions.
(C and D) Confocal images and statistic results of IF staining for H3K4me3 (C) and H3K27me3 (D) in WT and KO EAF stage oocytes. Scale bars, 10μm. (**) P<0.01, (***) P<0.001, n=6, Student's *t*-test.
(E) The upper panel showed IF staining results for H3K36me3 in *Sall4*$^{fl/fl}$ (WT) and *Sall4*$^{fl/fl}$*;Zp3-Cre* (KO) oocytes. Scale bars, 20um. The lower panel showed statistics analysis results of H3K36me3 levels in WT and KO EAF stage oocytes. Data represent mean ± SEM, n=6. (***), P< 0.001.

FIGURE 7. Proper levels of H3K4me3 and H3K27me3 are essential for oocytes maturation.
(A) IF staining for H3K4me3 and H3K27me3 of oocytes after injection manipulation for 7 days in control (Ctrl) and experimental (Exp) groups. Scale bars, 10 μm.
(B) Morphology of oocytes in control and experimental groups after maturation induction for 24 hours. Scale bars, 50 μm. Oocytes in the control group underwent GVBD and polar bodies were obvious in some

oocytes, whereas the germinal vesicles remained in most of the oocytes in the experimental group.
(C) Statistics analysis of GVBD rate in control groups and experimental groups. In total, 313 oocytes were injected in control groups and 332 oocytes were injected in experimental groups. Data represent mean ± SEM, n=3, (***) $P<0.001$, Student's *t*-test.
(D) Heat map of typically differentially expressed genes in all kinds of KO (or experimental groups) oocytes.
(E) ChIP-qPCR analysis of H3K4me3 and H3K27me3 levels on the promoter regions of oogenesis key genes. The upper panel showed the H3K4me3 enrichment levels on the promoter regions. The lower panel showed the H3K27me3 enrichment levels on the promoter regions. All enrichment values are relative to each input enrichment values, and then normalized with WT enrichment values. Data represent mean ± SEM, n=6 (6=2 ChIP replicates × 3 qPCR replicates), (***) $P<0.001$, (*) $P<0.05$, Student's *t*-test.

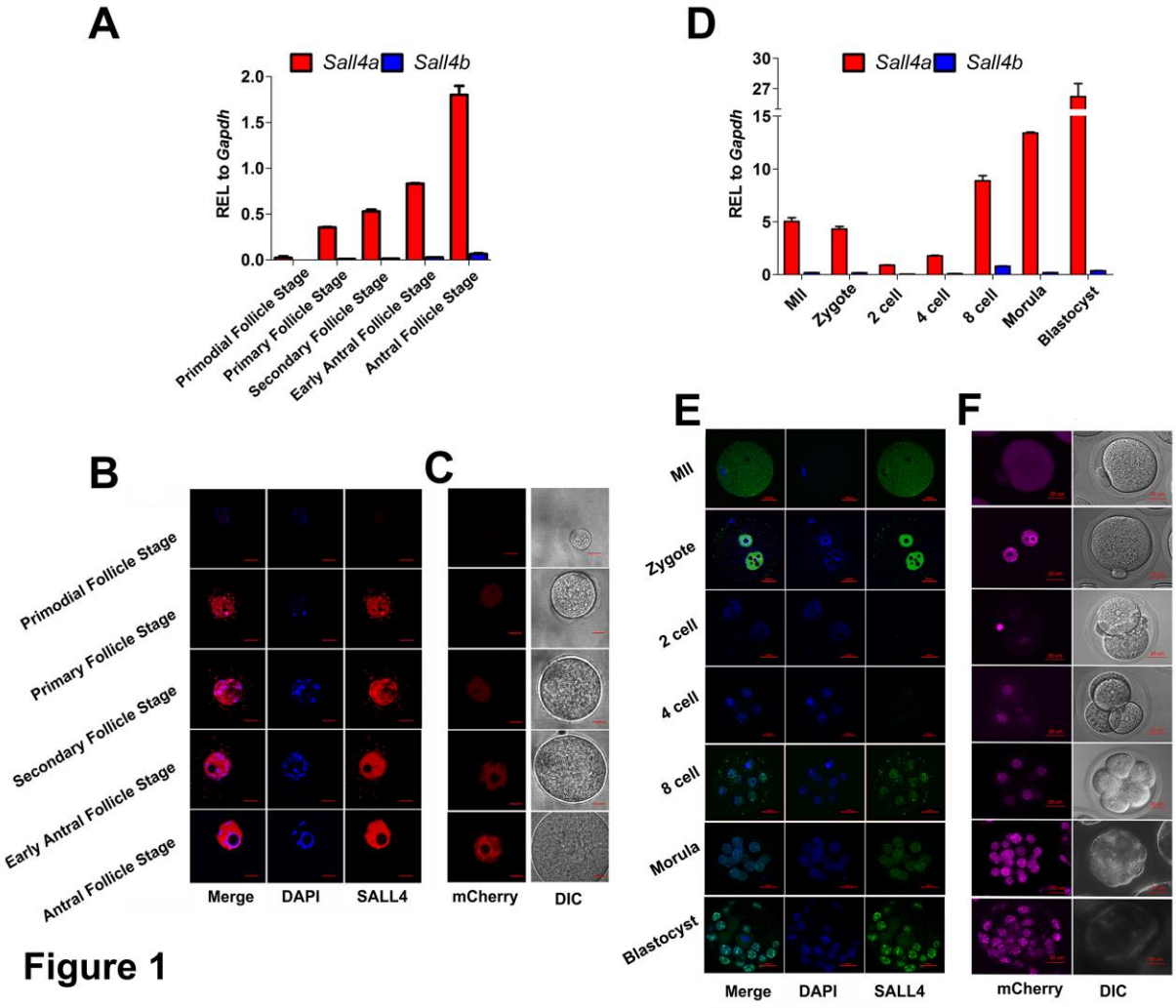

Figure 1

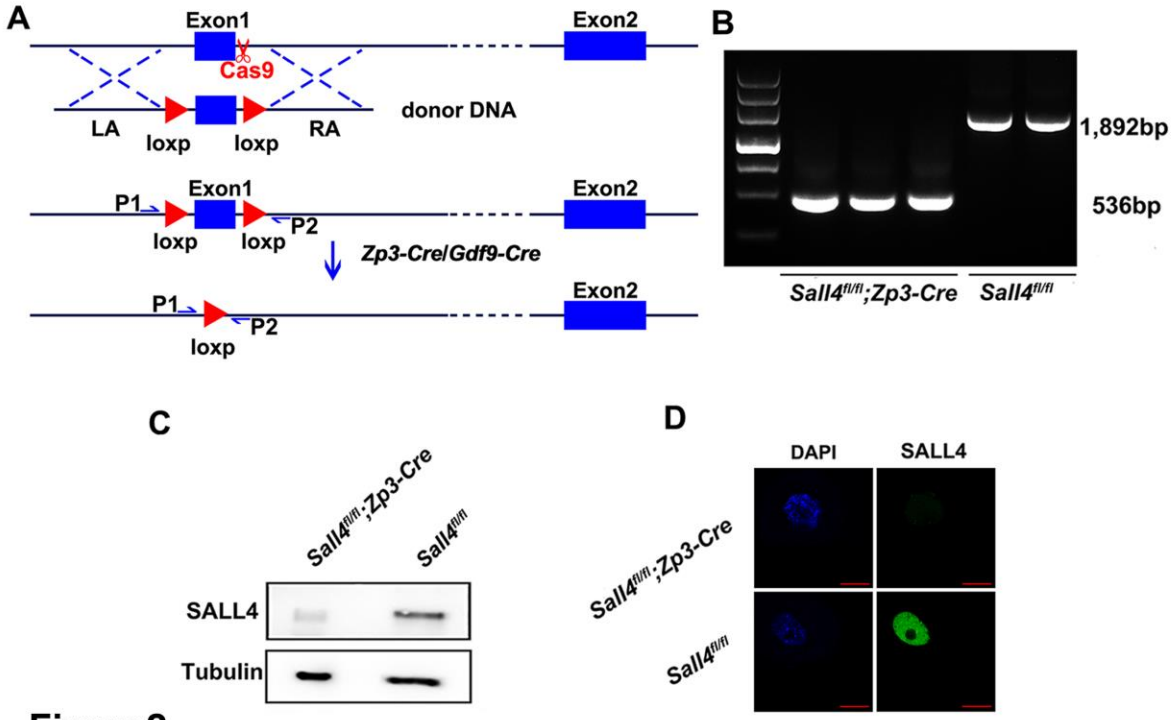

Figure2

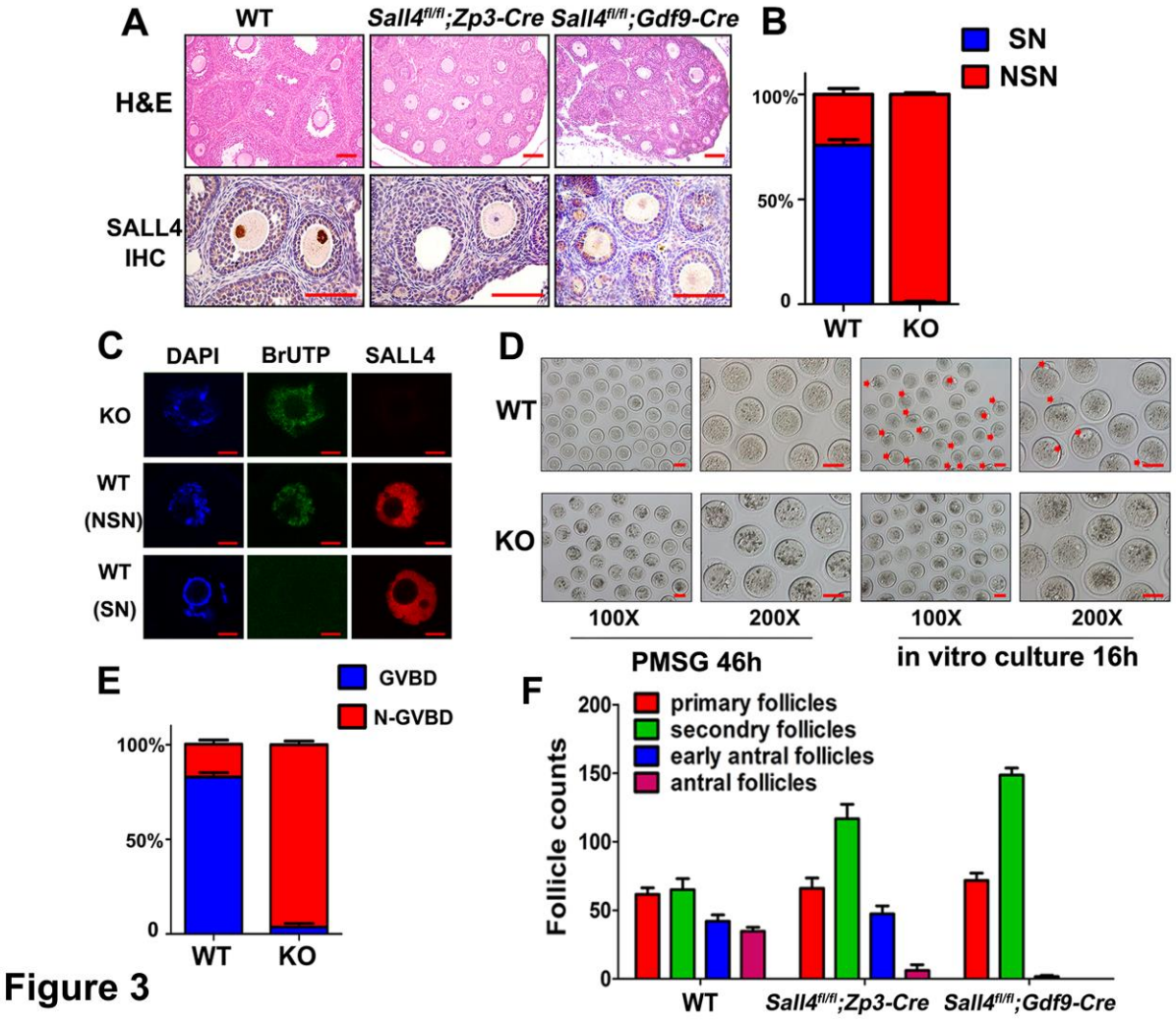

Figure 3

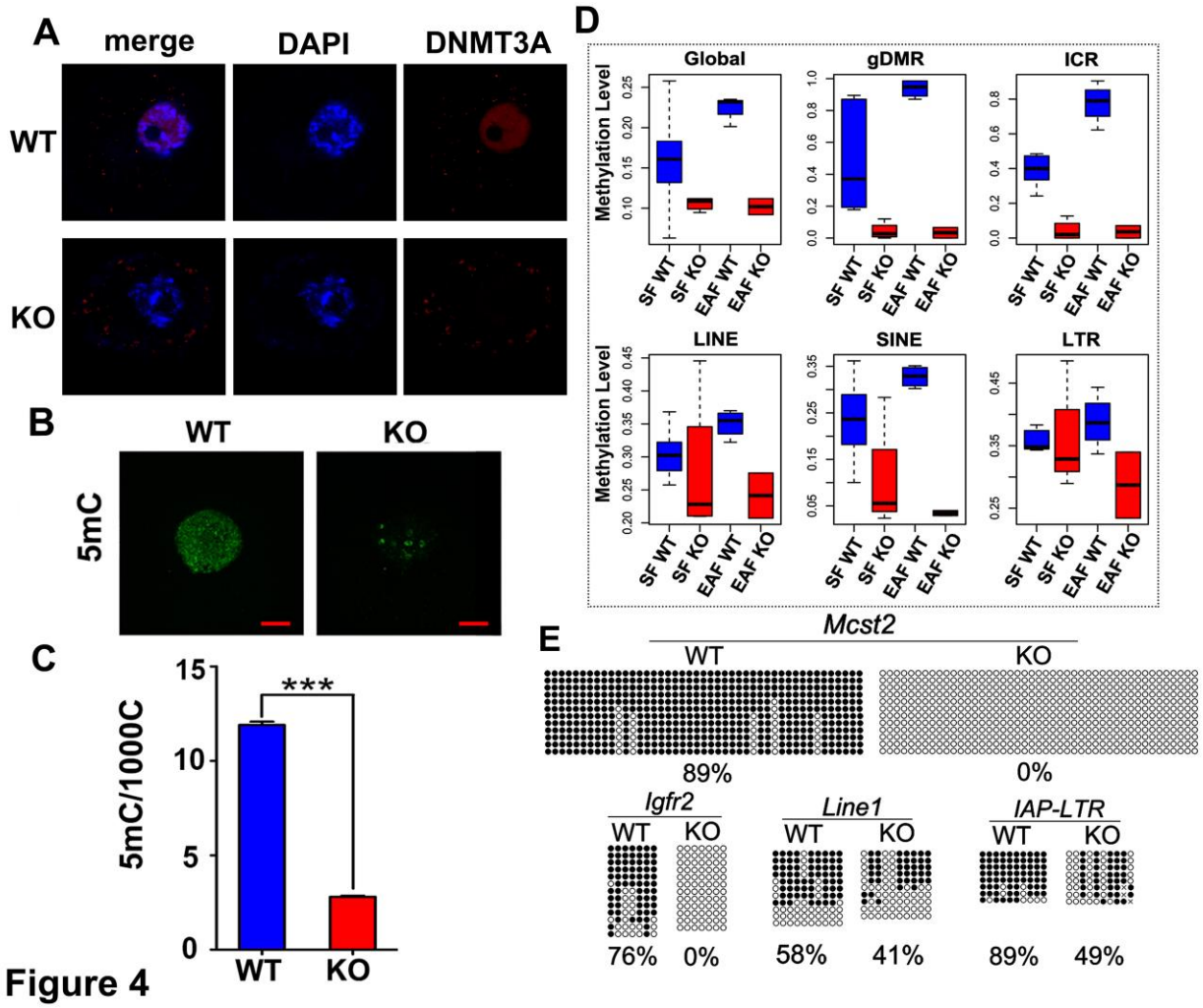

Figure 4

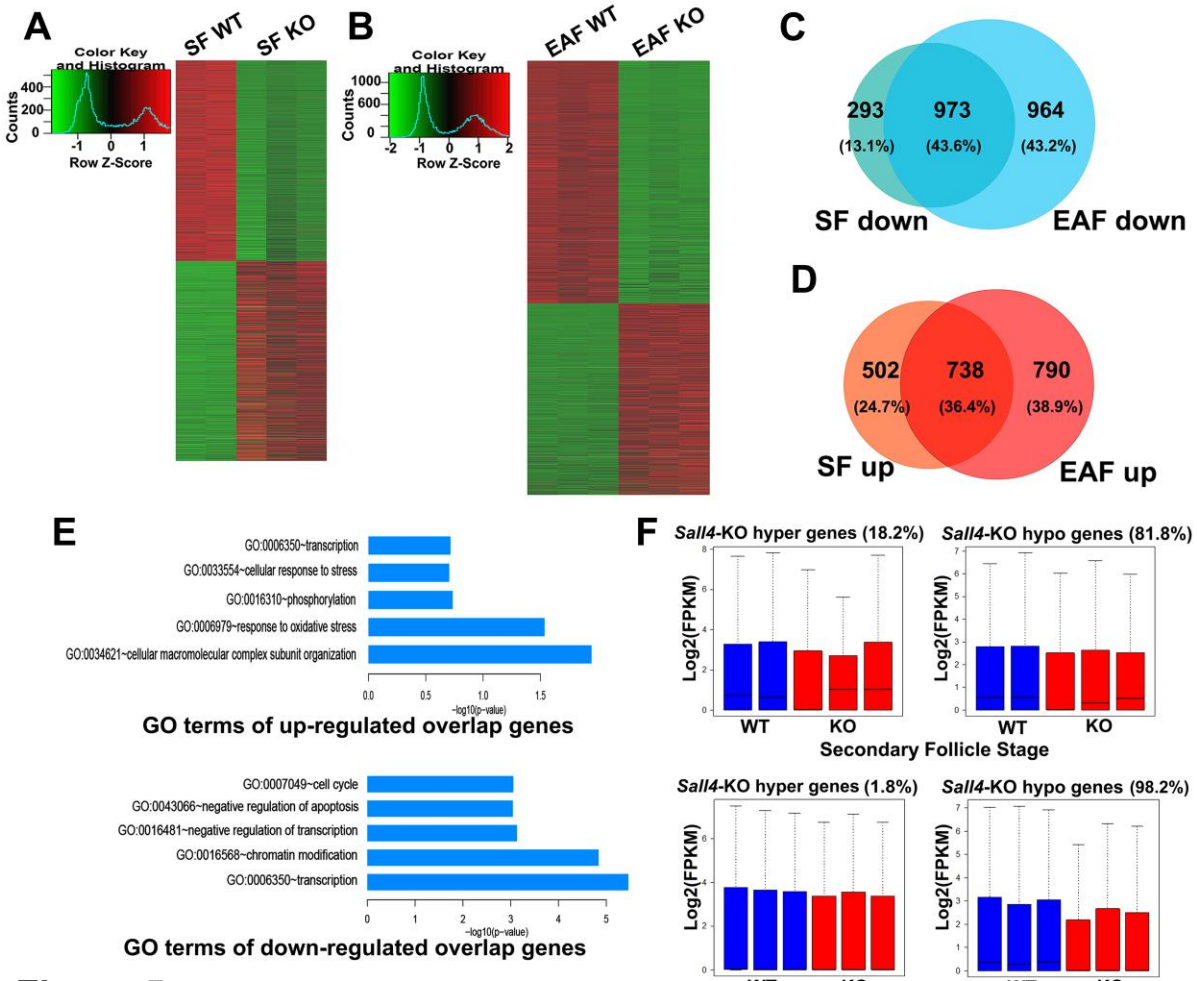

Figure 5

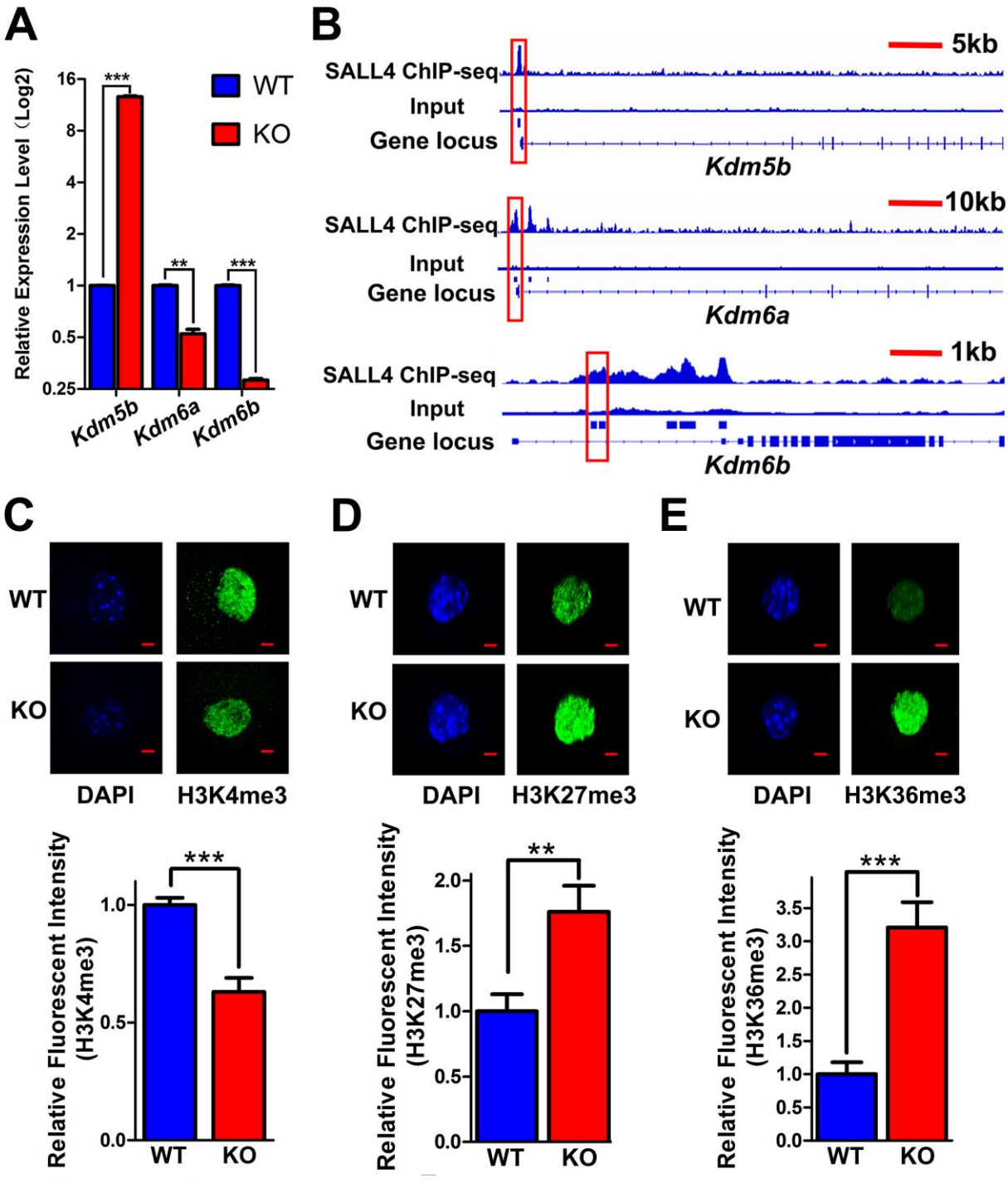

Figure 6

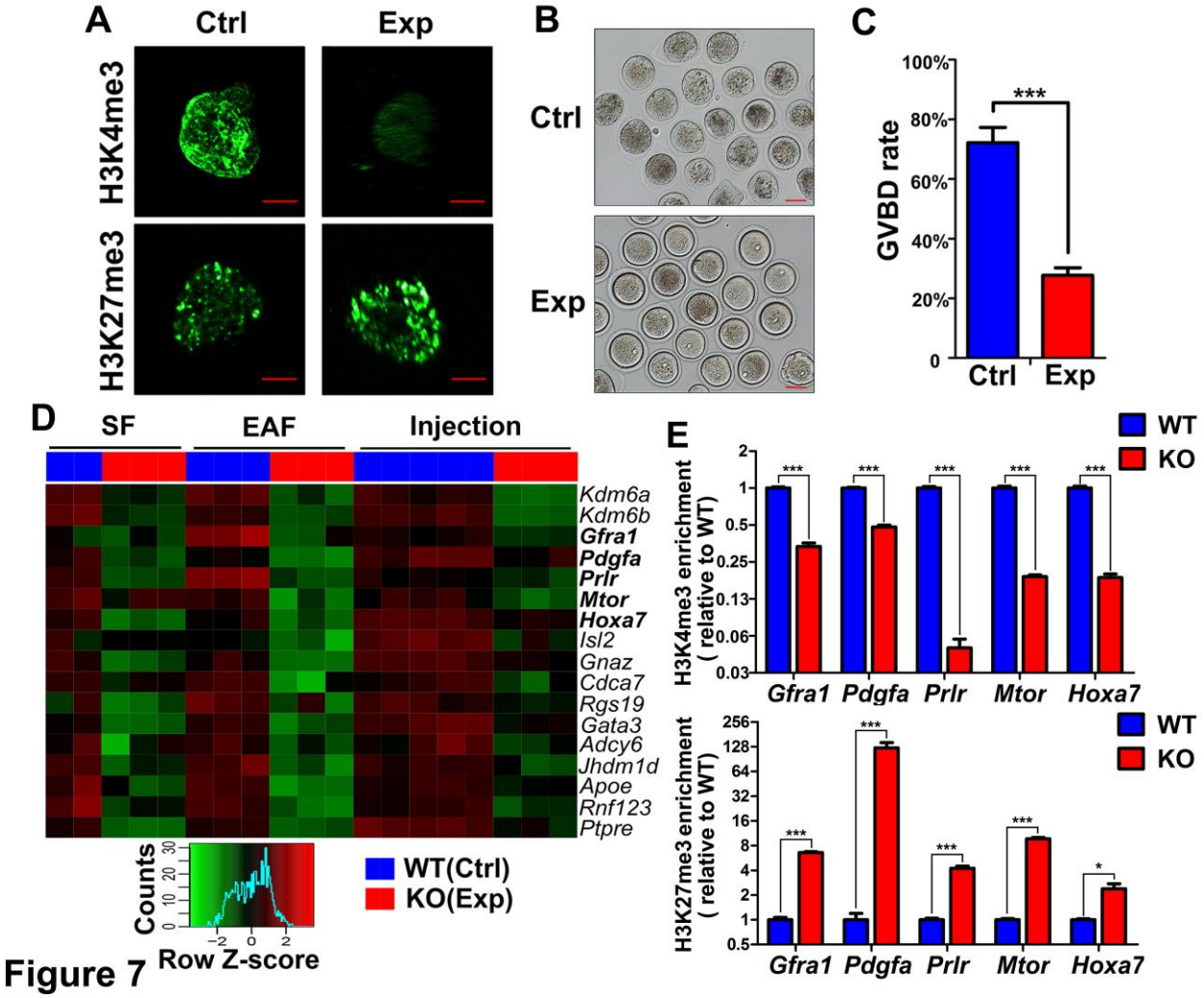

Figure 7

Maternal Sall4 Is Indispensable for Epigenetic Maturation of Mouse Oocytes

Kai Xu, Xia Chen, Hui Yang, Yiwen Xu, Yuanlin He, Chenfei Wang, Hua Huang, Baodong Liu, Wenqiang Liu, Jingyi Li, Xiaochen Kou, Yanhong Zhao, Kun Zhao, Linfeng Zhang, Zhenzhen Hou, Hong Wang, Hailin Wang, Jing Li, Hengyu Fan, Fengchao Wang, Yawei Gao, Yong Zhang, Jiayu Chen and Shaorong Gao

J. Biol. Chem. published online December 28, 2016
